Summer Student Report: W-Tagging/B-Veto in SUSY search for squarks and gluinos in final states with missing transverse energy, jets, and one isolated lepton at ATLAS

Max Reyer (Univ. Göttingen)

November 1, 2015

Abstract

This report recapitulates my stay at CERN as a Summer Student in a 13-week period from June 29 to September 25 in 2015. During that time, I was part of the CERN ATLAS Supersymmetry working group and working on a project exploiting W-tagging and B-veto techniques for the search for squarks and gluinos in final states with missing transverse energy, jets, and one isolated lepton.
In this report, I will summarize my project and present results and conclusions. Apart from that, I will also write about my experience with the Summer Student lectures, the social aspects and the CERN Summer School in general.

Contents

1 The project

1.1 Introduction

1.1.1 Supersymmetry (SUSY)

Supersymmetry (SUSY) introduces a new fundamental symmetry to the Standard Model (SM), which mixes the fermionic and bosonic sector together. As a consequence, one additional particle per SM particle, the so called *supersymmetric partner* (superpartner/sparticle), emerges. SUSY is assumed as a basis for more general theories like *M-theory* and can provide a *dark matter* (DM) candidate as well as a rather elegant solution to the so called *hierarchy-* or *fine tuning problem.* Furthermore, unification of the coupling constants at the GUT scale is feasible in the context of SUSY (cf. e.g. [8]).
Due to its beauty and importance, SUSY is considered as a promising candidate for beyond-the-standard-model (BSM) physics, which is hoped to be seen at the unprecedented energies[1] reached in the current run of the Large Hadron collider (LHC) and the high luminosities expected from the High-Luminosity-LHC (HL-LHC) upgrade in future. However, so far no evidence for SUSY could be observed. Thereby, many SUSY models could already be ruled out (e.g. SUSY with unbroken symmetry, exclusion of low-mass sparticles), primarily using the data from the 7TeV and 8TeV LHC-Run1 data.

1.1.2 Searching for SUSY

In supersymmetric theories, due to electroweak symmetry breaking, the pure superpartner states to the Higgs and electroweak bosons mix to form mass eigenstates. Specifically, the bino ($U(1)$ superpartner), neutral wino ($SU(2)$ superpartner) and neutral higgsinos (Higgs superpartners) form the four *neutralinos* $\tilde{\chi}_1^0, \tilde{\chi}_2^0, \tilde{\chi}_3^0, \tilde{\chi}_4^0$, while the charged winos and charged higgsinos form the charginos $\tilde{\chi}_1^\pm, \tilde{\chi}_2^\pm$ (cf. e.g.. [8]).
However, at hadron colliders like the LHC, processes mediated by the strong force are predominant. Hence, those particles are mainly produced in decay chains originating from primarily produced gluinos (gluon superpartners) or squarks (quark superpartners).
Assuming R-parity conservation, the lightest sparticle (LSP) is stable[2]. Often it is assumed to be the lightest neutralino $\tilde{\chi}_1^0$. Consequently, supersymmetric decay chains will end up with a stable $\tilde{\chi}_1^0$, which escapes the physical detector without leaving any trace (cf. fig. A.1). Hence large missing (unbalanced) transverse momentum ($\not{p}_T$) is an experimental sign for processes involving SUSY.
However, this signature is also produced by purely SM-events involving high momentum neutrinos, against which one consequently has to discriminate using certain selections and cuts on (kinematical) variables. Those cuts define *signal regions* (SR), which can be thought of as bins in a space spanned by the kinematical variables under scrutiny and which are expected to be especially

[1] 13 TeV centre-of-mass energy in proton-proton collisions
[2] Hence the name *'Lightest Stable Particle'*

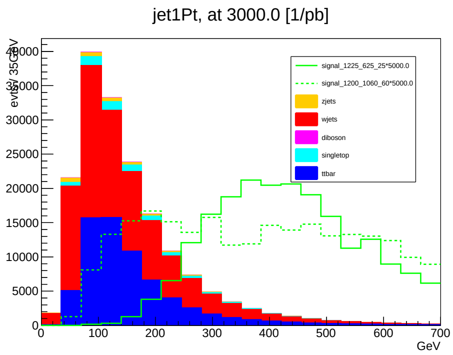

Figure 1.1: Comparison of the hardest jet p_T between BG and two SG models, after a certain preselection. The signals are enhanced for higher p_T. Note the scale factor for the signals.

enriched by SUSY processes (cf. fig. 1.1).

In those SRs, the SM background can be predicted by Monte-Carlo event generators (MC), or with data-driven background estimation techniques (and validated in different *validation regions* (VR)). After data taking, an excess in data events over the background prediction would hint to the presence of new physics. This excess is typically measured in *significance*[3]. In order to become more sensitive and conclusive, it is hence important to tune the SR for a better SG/BG ratio. This is typically done by utilizing SUSY-signal predictions from MC and varying the SR cuts in an optimization procedure to obtain maximal discovery significance. However, SUSY has lots of open parameters[4] (e.g. particle masses), on which the kinematics of the decays and hence the optimal SR definitions are directly dependent. As a consequence, multiple SR bins must be made, in order to account for a wide range of parameter sets.

1.1.3 Search for gluinos and squarks in final states with missing transverse energy, jets, and one isolated lepton

This analysis („strong 1-lepton“) approaches such SUSY processes, where a primarily produced gluino decays over an intermediate step, involving quarks and a chargino, into the LSP and accompanying W-bosons (cf. fig 1.2). More specifically, it selects events requiring one identified, isolated lepton. In that sense, the analysis addresses those processes, where one W is decaying into a lepton-neutrino pair ($W \to \nu_l l$), while the other W undergoes a hadronic decay ($W \to q\bar{q}$) and leaves two jets in the final state.

Background With this selection, the main BG consists out of $t\bar{t}$ and W+jet production (cf. fig. 1.3), which are both able to fake the signal by providing a hard lepton and missing $\not{p}_T$ by virtue of the escaping neutrino. There is also an analysis which requires two leptons and hence targets two leptonically decaying

[3] I.e. the level of significance corresponding to the p-value of the number of data events and the SM as null hypothesis (probability that the excess is just seen as an accident from the fluctuation of the BG).

[4] At least 124 independent ones.[7]

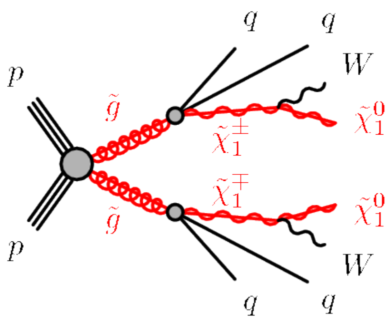

Figure 1.2: The SUSY process under scrutiny of the search for gluinos and squarks in final states with missing transverse energy, jets, and one isolated lepton [2].

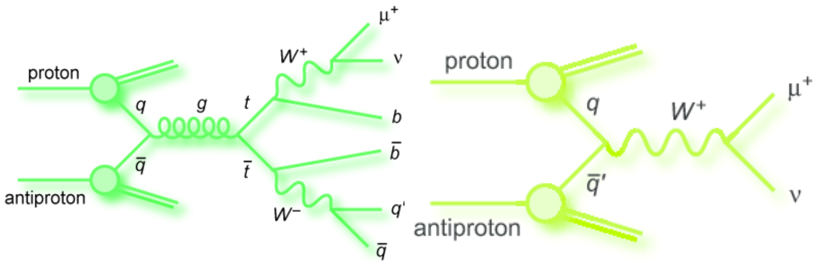

Figure 1.3: The main BG to the search: $t\bar{t}$ (left) and W+jets (right). Note that these diagrams are actually for proton-antiproton collisions, but due to the present antiquark content in high energy protons, they are also valid for pp collisions [6].

W as well as an analysis requiring no leptons at all. Those however give either very low BG but little statistics (two leptons), or large BG but high statistics (no leptons required). The 1-lepton analysis hence offers a tradeoff between statistics and background abundance.

Kinematic variables In order to form the SR described above, this analysis uses two additional, non-trivial kinematic variables to discriminate against the BG (cf. [2]). The *effective mass*:

$$m_{eff}^{lepton} = p_T^l + \sum_{jets} p_T^{jet} + \not{p}_T \tag{1.1}$$

is the sum of all accessible transverse momenta, including $\not{p}_T$. The SUSY signal process involves intermediate particles with much higher masses, hence this sum is expected to be much higher than for $t\bar{t}$ and w+jets.
In the signal model, the LSP, produced roughly back to back to the W, contributes to $\not{p}_T$. Hence, in the calculation of the *transverse mass*:

$$m_T = \sqrt{2p_T^l \not{p}_T (1 - \cos[\Delta\phi(\vec{l}, \not{p}_T)])} \tag{1.2}$$

it pushes the angle in the cos towards π and increases in turn m_T relative to the BG m_T.
The discrimination power of those variables is shown in fig. 1.4, where they are plotted without any applied cuts apart from the preselections.

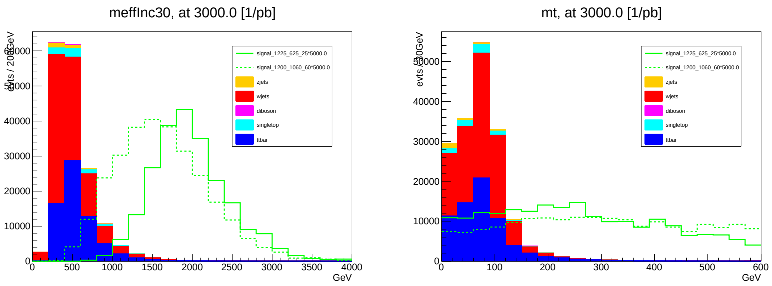

Figure 1.4: Comparison of m_{eff}^{lepton} (left) and m_T (right) between background and two signal models. Note the scale factor for the signals.

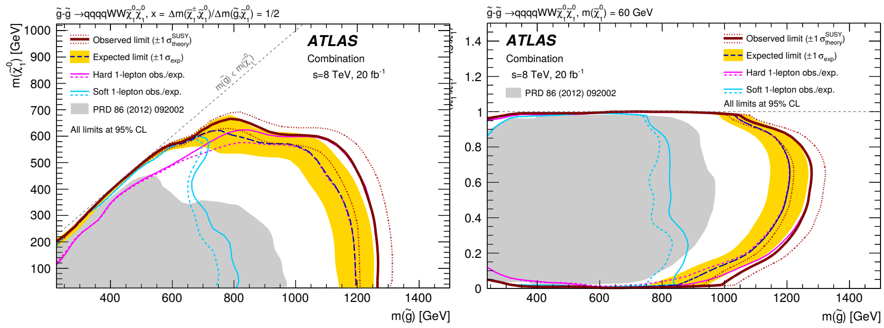

Figure 1.5: Exclusion plots for SUSY mass parameters in the $\tilde{g}\tilde{g} \rightarrow qqqqWW\tilde{\chi}_1^0\tilde{\chi}_1^0$ decay [3].

1.1.4 Target of the project

The kinetical energy of the W can be estimated to be proportional to the mass gap $\Delta m = m_{\tilde{\chi}_1^\pm} - m_{\tilde{\chi}_1^0}$ between chargino and neutralino. While this difference was rather small for the SUSY mass parameter sets tested (and excluded, cf. fig 1.5) in LHC-Run1, models with much larger Δm are accessible with the increased energy of $\sqrt{s} = 13$TeV in Run2 due to a dramatically increased $\tilde{g}\tilde{g}$-production cross section. In such models ('signal points'), we hence expect the W to be *boosted*, which leads to a small angular spacing of the decay products ($\propto 2m_W/p_T^W$, cf. e.g. [9]). As a consequence, the two jets originating from the hadronically decaying W will eventually overlap and could not be resolved by standard jet-reconstructing algorithms (e.g. with cone parameter $R = 0.4$) any longer.

However, most of the jet-pairs will completely lie inside a cone with a larger parameter (e.g.. $R = 1.0$), and are instead reconstructable as a single *fat jet*. The substructure of such a fat-jet originating from hadronical W-decay will be different from others, and therewith a tagging of such *W-jets* can be attempted. Since the collision energy needed for those kind of techniques has not been available so far, their exploitation is still in an early state. However, some first studies have already been carried out and serve as a prove-of-principle (cf. [1] for the ATLAS related studies).

Since the W+jets BG (after the 1 lepton requirement) doesn't feature a $W \rightarrow q\bar{q}$ decay, the requirement of a W-tagged fat jet could have power to eliminate this BG vastly. Especially in the upper right edge of the right plot in fig. 1.5, where

the mass splitting between chargino and neutralino is high and the W hence very boosted, a significant sensitivity enhancement could be anticipated. Another much more mature tagging technique (*b-tagging*) targets the identification of jets from b-quarks. Because signal events must not necessarily exhibit b-quarks in the final state, a veto on events with b-tagged jets could therefore improve the ratio between signal and $t\bar{t}$ BG. Especially the enhanced b-tagging capabilities of the upgraded ATLAS detector render a trial of it interesting.
The goal of the project thus was to utilize both tagging techniques described above to study their usefulness and power to increase the sensitivity of the analysis.

1.2 B-tagging studies

B-Jets exhibit a range of unique features, which can be used to discriminate them from other jets. Most prominent are the existence of a second vertex due to lagged decay of b-hadrons and and a wider jet-shape due to a mass gap between the b-quark and its decay products. Those features can be measured and combined to a overall variable using a multivariate technique. In this project, the so called *mv2-variable* was considered. It ranges between -1 and 1, indicating the probability of a jet to be a b-jet.
Cuts on this variable hence yield a decision whether a jet should be b-tagged or not. However, there are two different methods: One of them is the traditional fixed cut approach, where independent from the jet p_T a certain fixed mv2 threshold is used to do the tagging decision. Since the jet properties change with p_T, also the tagging efficiency[5] varies with p_T. The other method by contrast uses cut values dependent on the p_T of the jet under scrutiny, in order to compensate for the efficiency-variation. It aims for a flat-efficiency profile (over p_T) and is hence called *flat efficiency* b-tagging. Both methods were examined in this project and the findings presented below.

1.2.1 Fixed-cut B-tagging

As a first step, histograms of the number of b-tagged jets per event for the signal and the backgrounds were produced to gain insights into the possible discrimination power of a b-veto. Those plots are shown in fig. 1.6 for the ($m_{\tilde{g}}$ = 1200GeV, $m_{\tilde{\chi}_1^\pm}$ = 1060GeV, $m_{\tilde{\chi}_1^0}$ = 60GeV) SP and the $t\bar{t}$ BG, after the application of a quite loose SR cut. The different colours correspond to different b-tagging working-points, which use certain mv2-thresholds. The name of the WP indicate the efficiency which they were tuned for. As expected, WP of higher efficiency generally tag more b-jets. Furthermore, the $t\bar{t}$ BG shows much less events without tagged jets as the signal. Thus, the assumption of the presence of discrimination power could be confirmed. From the spacing between the numbers of events without tagged jets in signal and $t\bar{t}$ BG, it can already be anticipated that WP 70 should provide the best SG/BG ratio.

[5]Defined as (number of b-tagged jets)/(total number of b-jets)

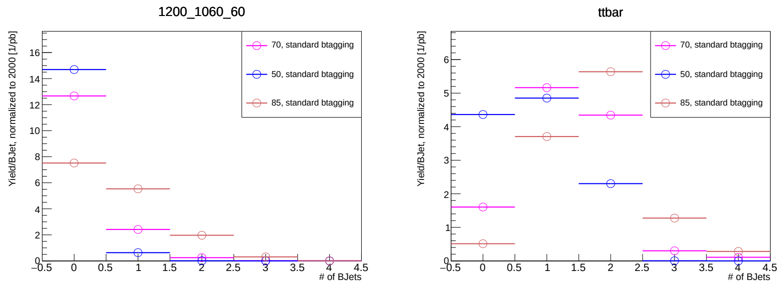

Figure 1.6: The histogrammed number of b-jets per event, normalized for 2fb^{-1}, after a quite loose SR cut. Lhs.: SP (1600, 1060, 60), Rhs.: $t\bar{t}$ BG.

var	cuts [GeV]
p_T^{j1}	150
p_T^{j2}	100
p_T^{j3}	50, 100
p_T^{j4}	50, 100
p_T^{j5}	50, 100

var	cuts [GeV]
m_T	250, 200, 150
$\not{p}_T$	150, 200, 250
m_{eff}^l	1200, 1400, 1600
p_T^{l1}	35
b-tag WP	NO,30,50,60,70,77,80,85,90

Table 1: Small optimization ranges of the first optimizations for the SP (1225, 625, 25).

Optimization After having the prove-of-principle at hand, the SR optimizations were carried out to determine the precise overall impact of the b-tagging to the analysis sensitivity.

The purpose of such an optimization is to find the optimal SR cuts, which yield the best discovery significance. Therefor, MC-samples for the signal and all backgrounds are used. For every SR of the optimization range, the yields of both SG and BG predictions, passing the respective SR-cuts, are evaluated. From those, the significance (z-value) of the predicted signal excess in the SR bin over the predicted background is estimated utilizing the Roostats NumberCountingUtils::BinomialExpZ tool. SR, where the uncertainty on the BG yield is larger than 30% of the total BG yield get vetoed in order to avoid too low MC statistics and too tight SR, faking high sensitivity. Eventually, the SR with the highest z-values can be read off to be the most sensitive ones.

At first, rather small optimization ranges (listed in tab. 1) of the kinematic variables were scrutinized together with the full set of fixed b-tagging WP (tab. 1 as well) for the SP (1225, 625, 25). The number of required (standard $R = 0.4$) jets was set to 5, the luminosity normalization of the used MC samples to 2fb^{-1}. The SR with the best performance plus the best SR not incorporating a b-tag veto are shown in tab. 2. Inside our optimization, an increase in sensitivity of more than 1.4σ could be observed.

To investigate the behavior of sensitivity and SG/BG ratio with varying b-tagging WP, ROC-curves were plotted for several fixed cuts on the kinematical variables as well as for fixed b-tagging WP. They can be found in fig. 1.7. Besides that, again for several fixed kinematical cuts, the optimal sensitivity per b-tagging WP was plotted and is shown in fig. 1.8, together with a plot showing the overall optimized significance for each WP (with optimal kinematical cuts

	Yields		cuts [GeV]									
Sign. [σ]	SG	BG	p_T^{j1}	p_T^{j2}	p_T^{j3}	p_T^{j4}	p_T^{j5}	$\not{p}_T$	m_T	m_{eff}^{l}	p_T^{l1}	b-tag WP
5.579	11.853	0.998	150	100	50	50	50	150	200	1600	35	70
5.569	11.667	0.966	150	100	100	50	50	150	200	1600	35	70
5.463	11.392	0.974	150	100	50	50	50	250	200	1400	35	70
4.112	11.582	2.378	150	100	100	100	50	250	200	1600	35	NO

Table 2: The three best overall SR plus the best SR without b-veto from the optimization over ranges from tab. for the SP (1225,625,25) and $\mathcal{L} = 2\text{fb}^{-1}$.

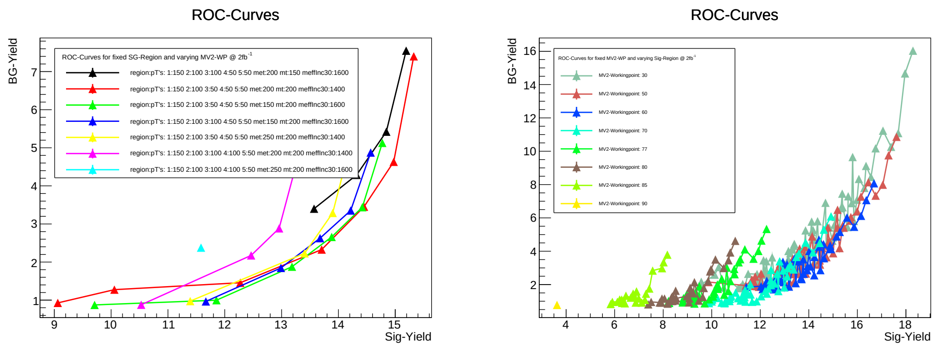

Figure 1.7: ROC-curves for the small optimization (tab. 1), for the SP (1225,625,25) On the left with fixed kinematical cuts and varying WP, on the right with fixed WP and varying kinematical cuts. WP 0 corresponds to no b-tag veto applied at all. The plots correspond to 2fb^{-1}. The single blue triangle represents the best SR without b-tagging.

per WP).

The study of the b-tagging impact on the single SP (1225,6325,25) was followed by the investigation of the SP corresponding to all available SUSY mass combinations . Since the plots and findings from the preliminary optimization trial for (1225,6325,25) indicate large sensitivity deteriorations for very high and very low WP, the subsequent optimizations were carried out with a reduced b-tag WP range, only including WP around 70 (cf. tab. 3). Furthermore, much larger optimization ranges were used (cf. tab. 3). For all SP, the optimizations were run for luminosities of $2, 4, 8, 20\text{fb}^{-1}$ and for the requirements of at least 4,5, and 6 jets harder than 30GeV. In order to be able to cope with the required computational power, a python-tool[6] was written which splits up the total range of SR into smaller chunks and submits the significance calculations for their SR as batch-jobs. Another script merges the output of the individual batch-jobs into one file, which in turn can easily be sorted by significance. Thus, it became feasible to perform optimizations with a range of SR as in tab. 3 in the order of half an hour.

The mass parameters from the set of examined SP follow two different schemes: Either the LSP-mass is fixed to 60GeV and chargino- and gluino-masses are varied, or gluino- and LSP-masses are variable, but the chargino mass is fixed as lying halfway between them. In both cases, the dependency of one of the mass parameter on the others can be used to plot certain SP-by-SP quantities in 2-dimensional grids. The first scheme is hence referred to as 'lsp60'-grid,

[6] To be documented separately.

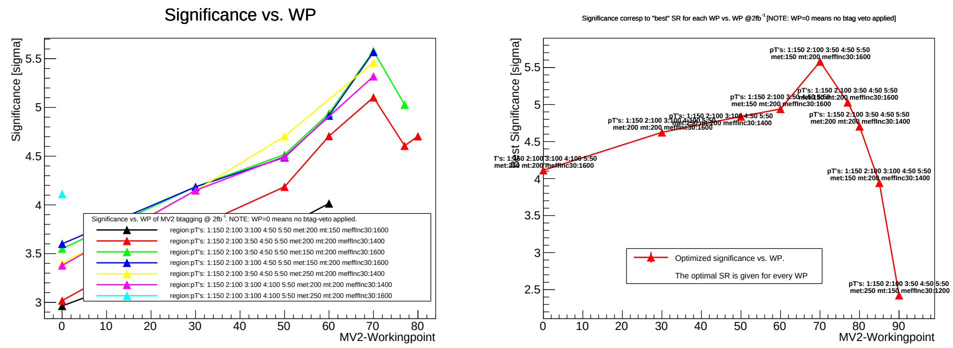

Figure 1.8: Significance per WP for the small optimization (tab. 1), for the SP (1225,625,25). On the left, for several fixed kinematical cuts, on the right with optimized kinematical cuts per each WP. Those optimized cuts are indicated at each marker. WP 0 corresponds to no b-tag veto applied at all. The plots correspond to 2fb^{-1}. The single blue triangle represents the best SR without b-tagging.

var	cuts [GeV]
p_T^{j1}	100,150,300
p_T^{j2}	25,50
p_T^{j3}	25,50
p_T^{j4}	25,50
p_T^{j5}	25,50

var	cuts [GeV]
m_T	250,200,150,120
$\not{p}_T$	150,200,250,300
m_{eff}^l	1000,1300,1600,1800
p_T^{l1}	35
b-tag WP	NO, 50, 60, 70, 77

Table 3: Large ranges for the optimization on batch, used for all SP.

whereas the latter one is called 'x05'-grid. The results of the optimizations are condensed in such 2-d mass grid plots in fig. 1.9-1.12.
Fig. 1.9 shows the best b-tagging WP per SP obtained from the point-by-point-optimization[7] described above. Again, the optimal WP was in most cases found to be 70, or at least to be close to it. This behaviour does not significantly change with the variation of the luminosity or the number of required jets.
In fig. 1.10 and 1.11, the optimized significance is plotted for both grids. Fig. 1.12 shows the impact of the b-veto as percental improvement. In either of the two cases, large improvements can be observed, which are quite dependent on the SP, though. This behaviour is again qualitatively quite similar at other luminosities and n_j, however the improvements seem to become more uniform over the grid at $n_j = 4$.

1.2.2 Flat-efficiency B-tagging

As already mentioned earlier, flat efficiency b-tagging uses mv2-thresholds dependent on jet p_T. Those cut-profiles are tuned in a way to ensure uniform efficiency over a certain p_T range. As for traditional b-tagging, several WP

[7] I.e. the additional cuts on the kinematic variables are not the same for every SP, but rather form (in combination with the b-tag veto of the plotted optimal WP) the optimal overall SR for this SP.

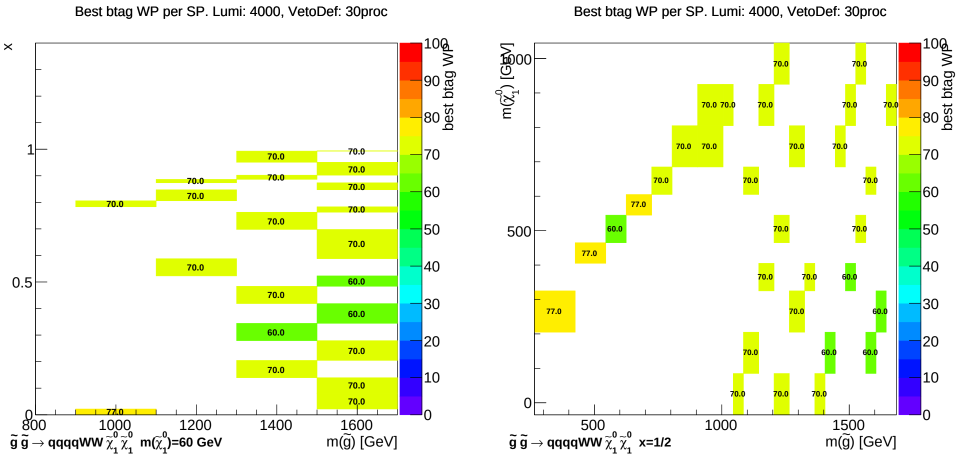

Figure 1.9: Best fixed-cut b-tagging WP from point-by-point optimization for the two mass grids. Here for $\mathcal{L} = 4\text{fb}^{-1}$ and $n_j = 5$.

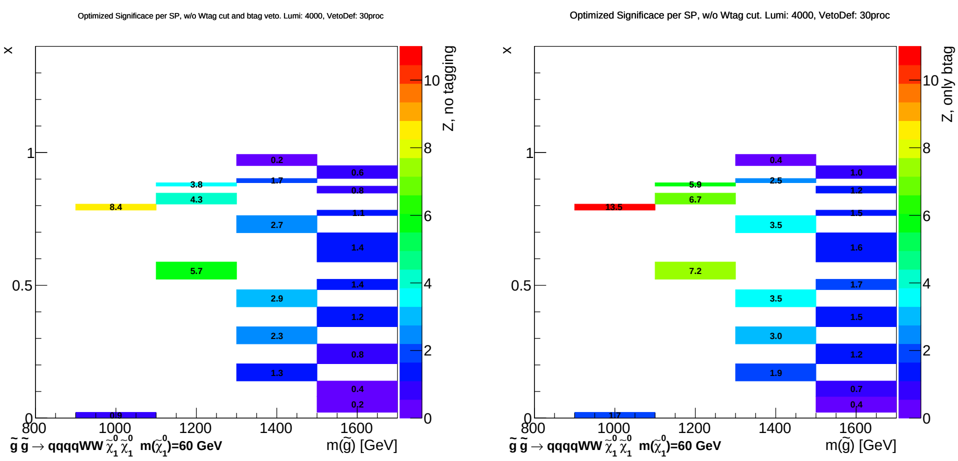

Figure 1.10: Comparison of the point-by-point optimized significance without (left) and with (right) b-veto for the lsp60-grid (The b-tag WP used per point is hence the same as shown in fig. 1.9). Here for $\mathcal{L} = 4\text{fb}^{-1}$ and $n_j = 5$.

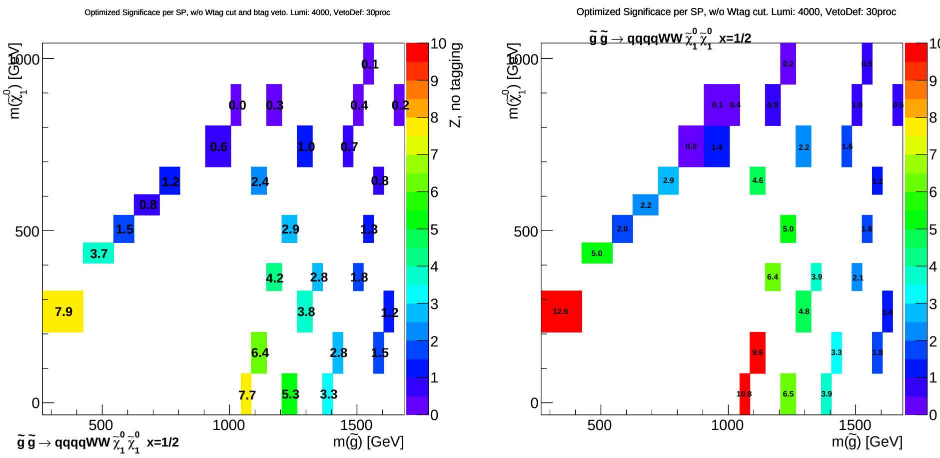

Figure 1.11: Comparison of the point-by-point optimized significance without (left) and wit (right) b-veto for the x05-grid (The b-tag WP used per point is hence the same as shown in fig. 1.9). Here for $\mathcal{L} = 4\text{fb}^{-1}$ and $n_j = 5$.

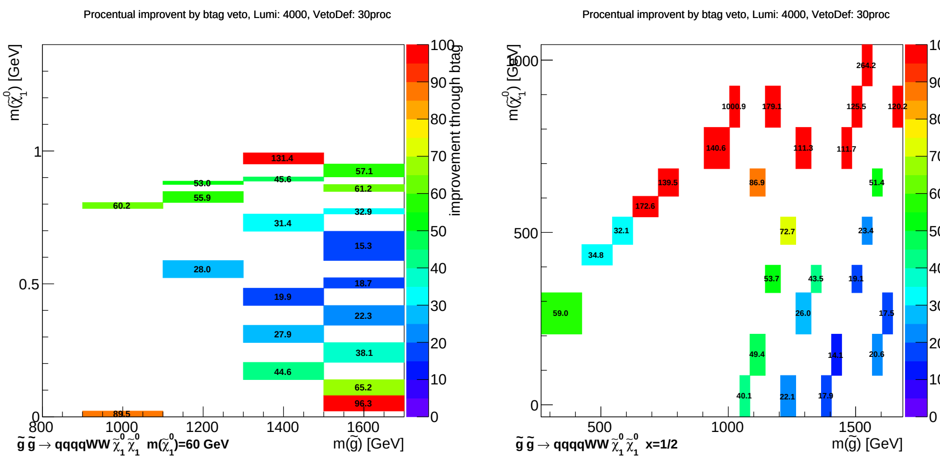

Figure 1.12: Percental by-point improvement in significance gained by the optimal by-point b-veto for the two mass grids. Here for $\mathcal{L} = 4\text{fb}^{-1}$ and $n_j = 5$.

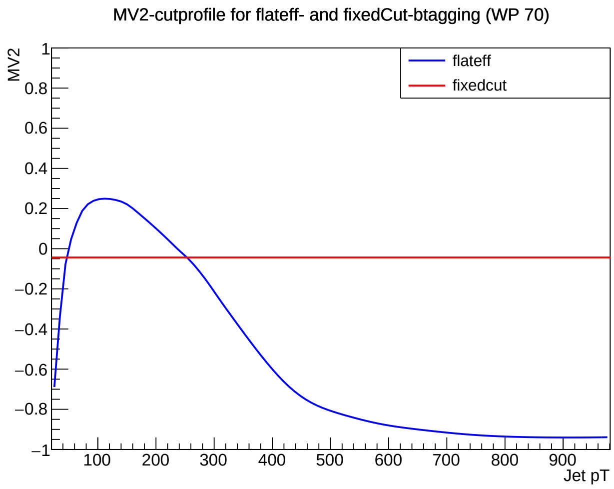

Figure 1.13: Cut-profile for flat efficiency b-tagging WP 70 compared to fixed cut for traditional b-tagging WP 70.

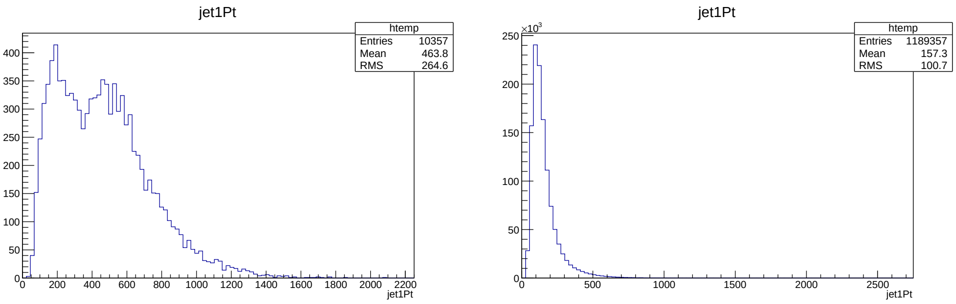

Figure 1.14: Comparison of the p_t^{j1} distribution in SP (1200,1060,60) (left) and $t\bar{t}$ BG sample (right). The double-peak structure in the signal originates from resolved and unresolved W-jets.

are defined, this time targeting certain flat efficiency values. An example for such a profile is shown in fig. 1.13. Since the threshold drops to small mv2 values at high p_T, a qualitatively quite different tagging behaviour can already be anticipated.

The same studies as for the standard b-tagging were carried out for flat-efficiency veto, yet only for a 5 jet requirement. Again, the optimal WP was found to lie in the region around 70 for all SP, and for all luminosities (c.f. fig. 1.15). Comparing the optimized significances with flat efficiency b-veto (fig. 1.16) with those from the standard b-veto optimization (fig. 1.10 and 1.11), we however observe a deterioration in sensitivity for almost all SP.
The reason for that can be found looking at the distribution of the leading jet transverse momentum of the SP- and $t\bar{t}$ BG samples (fig. 1.14). Due to the hadronical decaying boosted W, the p_t^{j1} is much higher for the signal sample, and lies largely in the region where the cut-profile drops to a very small threshold far beyond the fixed-cut value (fig. 1.13). At the same time, the vast majority of $t\bar{t}$ events has a p_T^{j1} which corresponds to cut-values elevated above the fixed cut value. Hence, less $t\bar{t}$ events get b-tagged, and consequently less BG vetoed,

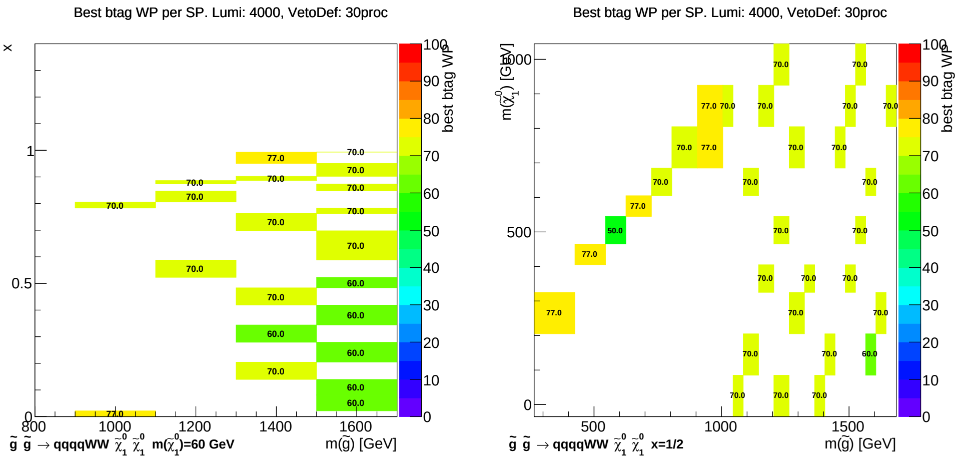

Figure 1.15: Best flat efficiency b-tagging WP from point-by-point optimization for the two mass grids. Here for $\mathcal{L} = 4\text{fb}^{-1}$ and $n_j = 5$.

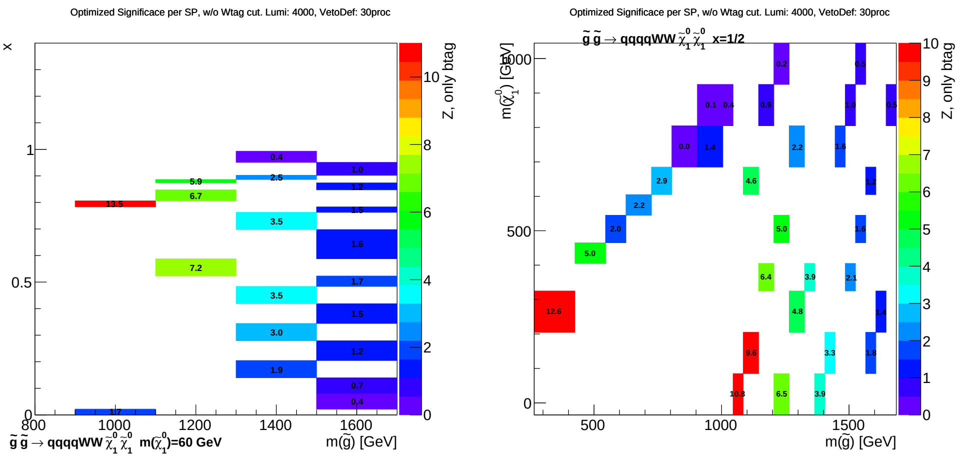

Figure 1.16: The point-by-point optimized significance with flat efficiency b-veto for both mass grids. Here for $\mathcal{L} = 4\text{fb}^{-1}$ and $n_j = 5$.

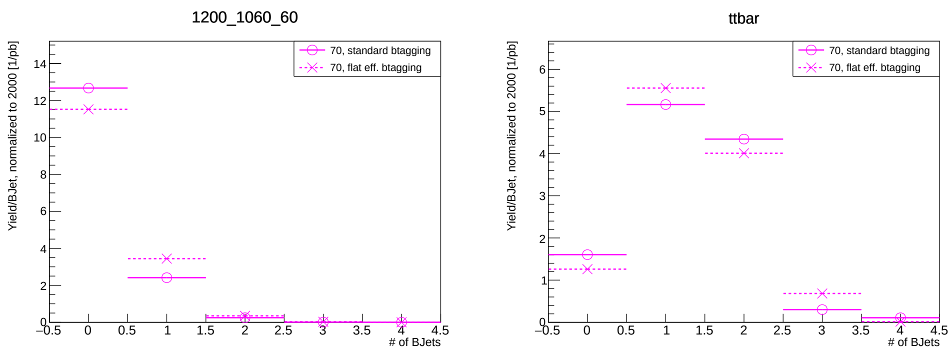

Figure 1.17: Comparison of the nBjet histograms for standard and flat efficiency b-tagging.

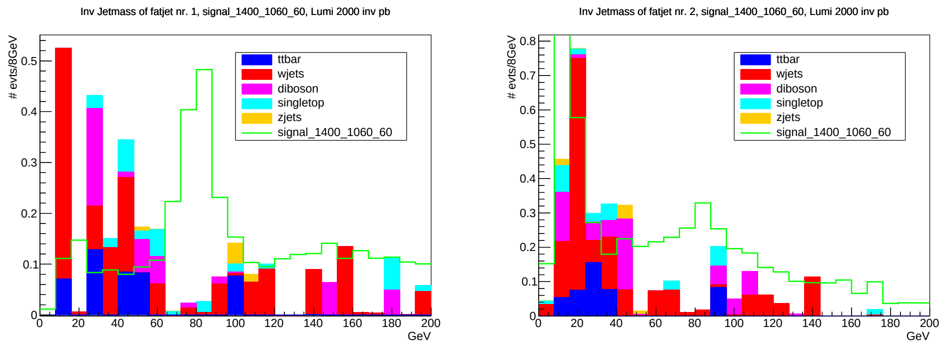

Figure 1.18: The invariant jet-mass distribution of the hardest (left) and second hardest (right) trimmed fat-jet of the SP (1400,1040,60), compared to the BG after the application of a quite loose SR cut with a b-tag veto.

whereas the high-p_T jets from the boosted W easily get mistaken as b-jets, such that in total more signal events get vetoed. This can also be nicely seen in fig. 1.17. Ultimately, the SG/BG-ratio and thus the significance decreases relative to the standard b-tagging technique.

1.3 W-tagging studies

As already mentioned in the introduction, W-tagging targets the evaluation of fat-jet-properties in order to discriminate those originating from hadronical W-decays against those from other sources. Instead of using fat-jets reconstructed directly from the topological clusters like in [1], the already reconstructed standard jets (R=0.4) were used as input for an anti-k_t clustering with R=1.0 to obtain *reclustered* fat-jets like proposed in [9]. This has the advantage, that jet calibration and uncertainties on the re-clustered p_T and invariant mass can be obtained from those of the standard jet. The reclustered fat-jets then got trimmed by removing constituents with a momentum contribution of less than 5% to remove pile-up and underlying-event contributions (c.f. [1]), and the invariant mass of the trimmed fat-jets was calculated.

A plot of the invariant trimmed fat-jet mass of the two hardest fat-jets for the SP (1400,1060,60) is shown in fig. 1.18. The hardest fat-jet mass peak for the W-mass in the signal is clearly visible and seems to discriminate very sharply against the BG (the expected peak in the $t\bar{t}$ sample is not visible, since $t\bar{t}$ is already largely killed by the b-veto). Also in the second hardest fat-jet mass a peak-like excess of the SG over the BG can be seen, coming from events where the fat-jet related to the W-decay is not the hardest jet. However, most events have rather small mass, originating from the jets emerging in the first decay in fig. 1.2.

As also done by [1], the most straightforward W-tagging technique would hence be a simple cut on the trimmed, reclustered fat-jet mass $m_{\text{recl,tr}}^{\text{fat-jet}}$. First tries targeted window-like cuts solely on the first fat-jet mass with a certain 'radius' Δm around the W-mass set to $m_W = 80.4$GeV (require $m_W - \Delta m < m_{\text{recl,tr}}^{\text{fat-jet1}} < m_W + \Delta m$). This could be slightly improved by involving also the second fat-jet, via requiring the jet-mass of the first *or* second hardest fat-jet mass to lie within such a

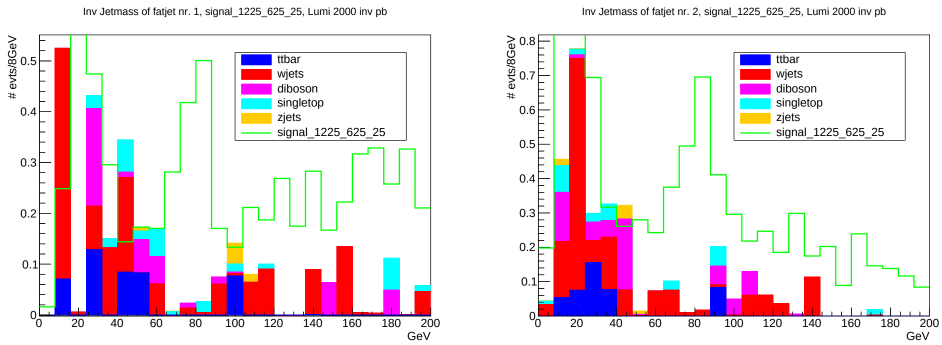

Figure 1.19: The invariant jet-mass distribution of the hardest (left) and second hardest (right) trimmed fat-jet of the SP (1225,625,25) compared to the BG after the application of a quite loose SR cut with a b-tag veto.

window. This addition gets even more important for points with larger spacing between $m_{\tilde{g}}$ and $m_{\tilde{\chi}_1^\pm}$ and smaller gap between $m_{\tilde{\chi}_1^\pm}$ and $m_{\tilde{\chi}_1^0}$, since the W fat-jet is more likely to not be the hardest fat-jet (jets from the first decay in fig. 1.2 grow more energetic). Such a SP (i.e. (1225,625,25)) is shown in fig. 1.19. It is apparent that the peak in the second fat-jet mass is significantly sharper compared to the SP from fig. 1.18. Besides the peak-structure, there is also a elevation at small mass for $m_{\text{recl,tr}}^{\text{fat-jet1}}$ since the W-jets and the jets from the first decay are energetically stronger mixed.

Nevertheless, optimizations using the describes W-tagging technique and various window sizes Δm could not reach the significances obtained by optimizations without W-tagging requirement, since the window-cut was too aggressive to the statistics. A further improvement was eventually made through performing only left-sided cuts on the jet mass (which removes the BG-pile at low $m_{\text{recl,tr}}^{\text{fat-jet}}$), as a tradeoff between optimal SG/BG ratio and sufficient statistics.

With this adjustment, the optimizations carried out with the ranges from tab. 3 plus $\Delta m \in \{NO, 20\text{GeV}, 25\text{GeV}, 30\text{GeV}, 40\text{GeV}\}$ started to show an impact of the W-tagging on the sensitivity.

In order to investigate the W-tagging behaviour and the dependence on the Δm 'WP', n-1 plots were made. Therefor, the cuts on all SR variables were fixed to some values, while the WP of the W-tagging (Δm) was varied. For each configuration, the yields for SG and the BG as well as the significance expectation were calculated as in the optimization procedure and plotted against Δm. The plots are shown for $\mathcal{L} = 4\text{fb}^{-1}$ and $\mathcal{L} = 20\text{fb}^{-1}$ in fig. 1.20. The black lines in the significance plots indicate the sensitivity obtained with the same cuts on the other (fixed) variables, but without W-tag cuts. The shaded area mark the WP for which the MC-statistics requirement (BG-uncertainty $< 30\%$ of total BG) is not fulfilled. From the plots can be concluded, that the effect of the W-tagging should become quite significant, at least for high luminosities and SP with a highly boosted W. However, the MC-statistics requirement seemed to be too strict for this study. Hence, an alternative statistics veto, requiring at least one MC-event of both $t\bar{t}$ and W+jets BG was defined and the optimizations carried out again. The results are presented in fig. 1.21-1.23. Although the

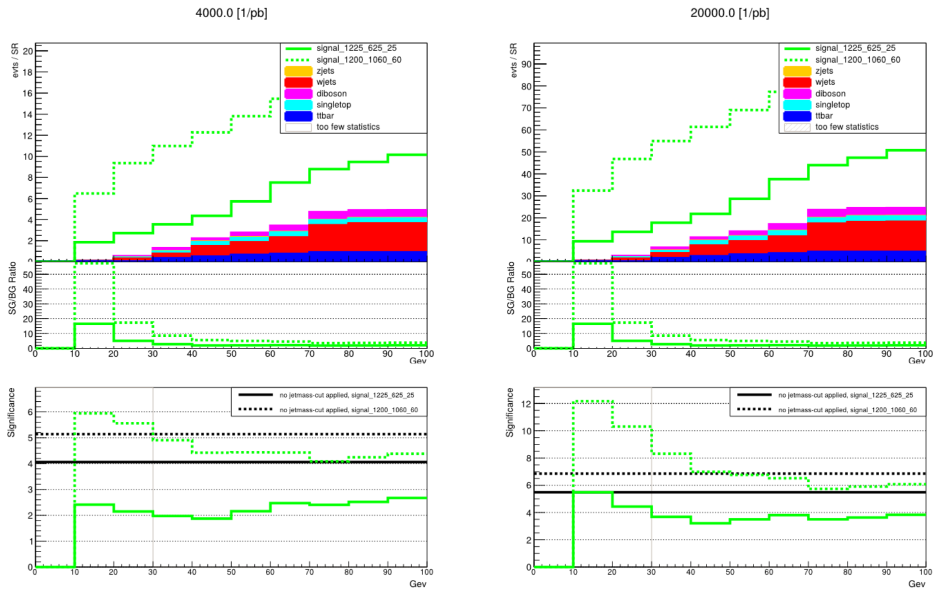

Figure 1.20: N-1 plots for the (onesided) W-tagging WP Δm, for $\mathcal{L} = 4\text{fb}^{-1}$ (left) and $\mathcal{L} = 20\text{fb}^{-1}$ (right). The required jet multiplicity is $n_j = 4$. The black lines indicate the sensitivity obtained with the same cuts on the other (fixed) variables, but without W-tag cuts.

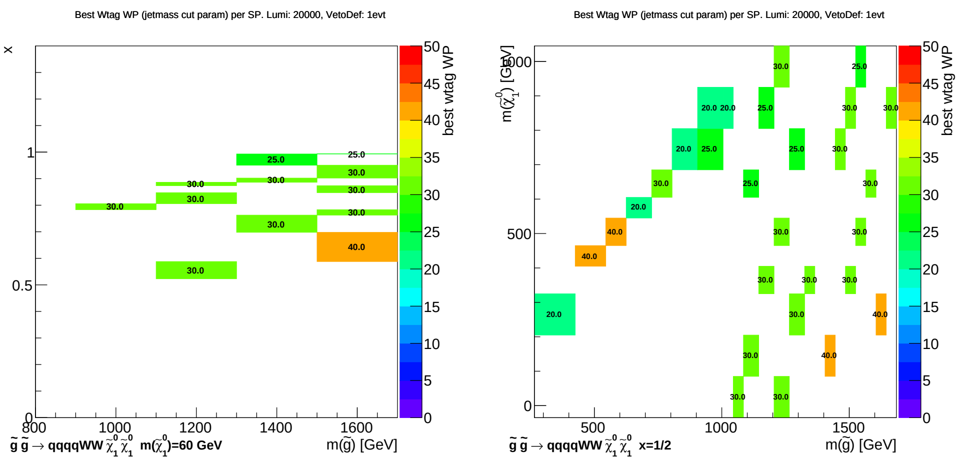

Figure 1.21: Best (onesided) W-tagging WP from point-by-point optimization for both grids. Only SP where the W-tag actually brings an improvement are shown. $\mathcal{L} = 20\text{fb}^{-1}$, $n_j = 5$.

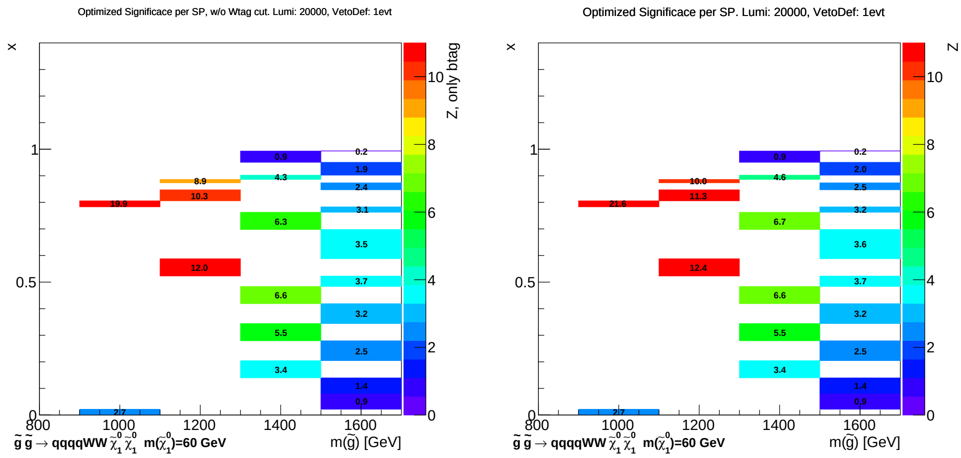

Figure 1.22: Comparison between the (point-by-point) optimized significance achieved without (left) and with (right) W-tagging (onesided) for the lsp60 grid. $\mathcal{L} = 20\text{fb}^{-1}$, $n_j = 5$.

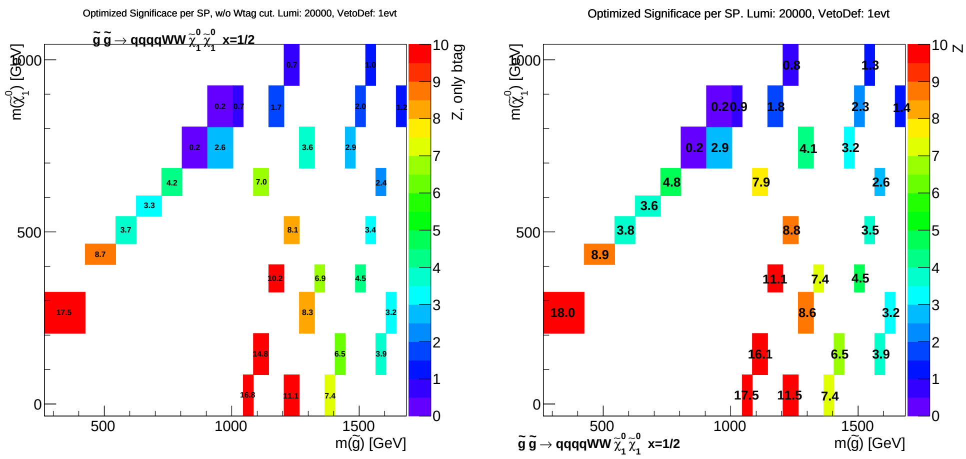

Figure 1.23: Comparison between the (point-by-point) optimized significance achieved without (left) and with (right) W-tagging (onesided) for the x05 grid. $\mathcal{L} = 20\text{fb}^{-1}$, $n_j = 5$.

plots show improvements for the application of the W-tag requirement, especially in the regions of higher W boost, they are however quite small. There are also some rather puzzling features, e.g. the enhancement of the significance close to the diagonal, where no boost is expected.
To conclude, it has to be said that W-tagging for the 1-lepton SUSY analysis has to undergo further investigation to become interesting for an application. Other substructure variables interesting for W-tagging, as summarized and examined by [1], were not considered in this project, as they would imply further decrease of tagging efficiency and hence aggravate the statistics even more (Since they are applied only after a cut on $m_{\text{recl,tr}}^{\text{fat-jet}}$. Yet, they could become important for SP with even higher boost, for which nevertheless much more luminosity is required.

1.4 Conclusion

In this project, it was shown that the utilization of a b-tag veto is able to enhance the sensitivity of the strong 1-lepton analysis for the 13TeV Runs of the LHC, while the implementation of a W-tag requirement implied certain complications and could not significantly enhance the analysis for most SP. A subsequent study of flat-efficiency b-tagging actually yielded that it performed worse than the traditional fixed-cut tagging. However, the nice shape (eg. fig. 1.18) of the W peak in the invariant mass plot could be tried to be used for certain methods. This is currently under further investigation within the working group.

2 The Summer Student Program

It really was an amazing opportunity to be able to take part in this years CERN summer school. Of course, I was quite exited when I received the acception for the program, and my expectations were not belied.

First weeks and the lecture series Especially the first weeks were extremely intense, but equally thrilling. Most of the lectures were really interesting and inspiring, and it was nice to discuss about them in the discussion sessions or later at lunch with the other summer students. They offered really nice insights into a broad range of topics around particle physics. Particularly the lecture of Yuval Grossman of has to be pointed out as outstanding. However, I must say that some courses became a bit too technical and hard to follow, especially some of those related to hardware.
The atmosphere among the Summer School participants was amazing, every night you could readily find a group to hang out and do stuff with, and on the weekend it was easy to find people to travel around. I made so many good friends, with whom I had an amazing time here at CERN, in Geneva, and all around Switzerland.

The workshops During my stay here at CERN, I had the opportunity to participate in a number of workshops. They definitely belong to the best experiences of the Summer School. Their hands-on approach offered a lot of fun, and a lot of insights behind the grey theory. Especially the scintillating crystals workshop must be pointed out. It was held by Carmelo, who did a great job in encouraging us to think deeply about the small experiment we carried out there. It was truly inspiring! Also the beamline workshop was great fun, where we were able to play around with one of the actual beamlines and hence learned a lot about collimation, targets, focusing and the creation of dedicated beams.

The project The project was probably the biggest part of the program, and definitely the part from which I learned the most. It was a great experience to be able to work in one of the ATLAS groups, to attend meetings and to learn about the organizational structure. I gained a lot of experience and numerous techniques by working on the project itself, and got more insight into the general structure of analyses in HEP. Besides that, regularly presenting slides in the group about the status of my project (and of course the presentation in the summer student session) was a nice exercise.

3 Acknowledgement

I want to thank CERN as a whole, and especially the Summer Student team constituted from Jennifer Dembski, Sharon Hobson and María José Morales Bazán. They did a great job in organizing workshops, social events and of course the student session as well as providing us with help and information. In that way, they enabled us a truly unforgettable summer.
Thanks also to all workshop organizers, especially to Carmelo, whose workshop (scintillating crystals) I won't forget in a long time.
Special thanks are due to my supervisor Moritz Backes, who provided me with a very interesting project, who gave me outstanding guidance and provided me with help whenever needed, also for questions not related to the project. Thanks for giving me a lot of freedom in working on the project!
Also many thanks to the 1-lepton and CATSUSY group, in whose meetings I had the opportunity to present my work regularly and where I received numerous useful comments. In that sense, I want to point out: Matthew Gignac, who helped me a lot with the analysis-framework; Ben Nachman, who supported me with the reclustering and provided me with the necessary code; Nils Ruthmann, who gave the idea to pursue flat-efficiency b-tagging, who provided me with lots of technical support and who answered me dozens of questions.
Last but not least, huge thanks to all the other Summies, especially to my new friends, for all the funny nights, adventures and travels, and in general for making this summer so great! I hope we will all stay in touch somehow.

A Appendix

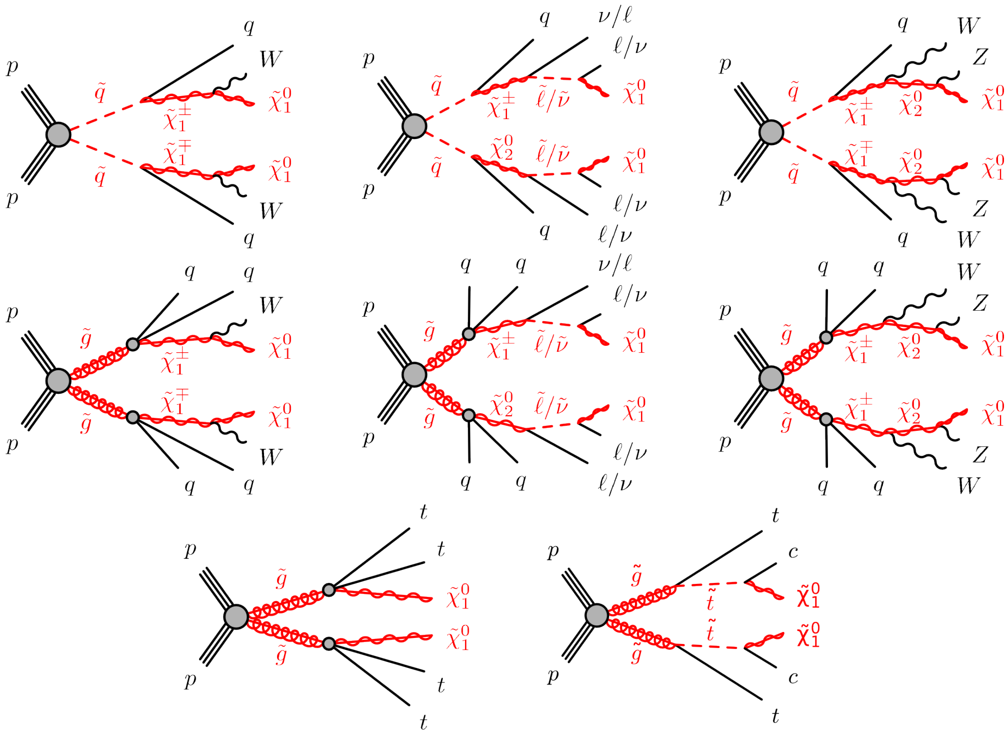

Figure A.1: Various (simplified) SUSY decay chains from a primary strong process, with LSPs in the final states [3].

References

[1] Performance of Boosted W Boson Identification with the ATLAS Detector. Technical Report ATL-PHYS-PUB-2014-004, CERN, Geneva, Mar 2014.

[2] Expected sensitivity studies for gluino and squark searches using the early LHC 13 TeV Run-2 dataset with the ATLAS experiment. Technical Report ATL-PHYS-PUB-2015-005, CERN, Geneva, Mar 2015.

[3] Georges Aad et al. Search for squarks and gluinos in events with isolated leptons, jets and missing transverse momentum at $\sqrt{s} = 8$ TeV with the ATLAS detector. *JHEP*, 04:116, 2015.

[4] A. Altheimer et al. Boosted objects and jet substructure at the LHC. Report of BOOST2012, held at IFIC Valencia, 23rd-27th of July 2012. *Eur. Phys. J.*, C74(3):2792, 2014.

[5] Matteo Cacciari, Gavin P. Salam, and Gregory Soyez. The Anti-k(t) jet clustering algorithm. *JHEP*, 04:063, 2008.

[6] DØ Experiment. Experiment website. `http://www-d0.fnal.gov/`, 2015.

[7] David Griffiths. *Introduction to elementary particles*. 2008.

[8] Stephen P. Martin. A Supersymmetry primer. 1997. [Adv. Ser. Direct. High Energy Phys.18,1(1998)].

[9] Benjamin Nachman, Pascal Nef, Ariel Schwartzman, Maximilian Swiatlowski, and Chaowaroj Wanotayaroj. Jets from Jets: Re-clustering as a tool for large radius jet reconstruction and grooming at the LHC. *JHEP*, 02:075, 2015.